Effect of AlN nucleation layer growth conditions on buffer leakage in AlGaN / GaN high electron mobility transistors grown by molecular beam epitaxy (MBE)

C. Poblenz, P. Waltereit, S. Rajan, U. K. Mishra, J. S. Speck, P. Chin, I. Smorchkova, and B. Heying

Citation: Journal of Vacuum Science & Technology B: Microelectronics and Nanometer Structures Processing, Measurement, and Phenomena **23**, 1562 (2005); doi: 10.1116/1.1943443

View online: https://doi.org/10.1116/1.1943443

View Table of Contents: https://avs.scitation.org/toc/jvn/23/4

Published by the American Institute of Physics

ARTICLES YOU MAY BE INTERESTED IN

Effect of carbon doping on buffer leakage in AlGaN/GaN high electron mobility transistors
Journal of Vacuum Science & Technology B: Microelectronics and Nanometer Structures Processing, Measurement, and Phenomena **22**, 1145 (2004); https://doi.org/10.1116/1.1752907

Influence of AlN nucleation layer temperature on GaN electronic properties grown on SiC
Applied Physics Letters **80**, 4372 (2002); https://doi.org/10.1063/1.1484553

Influence of AlN nucleation layers on growth mode and strain relief of GaN grown on 6H–SiC(0001)
Applied Physics Letters **74**, 3660 (1999); https://doi.org/10.1063/1.123214

Two-dimensional electron gases induced by spontaneous and piezoelectric polarization charges in N- and Ga-face AlGaN/GaN heterostructures
Journal of Applied Physics **85**, 3222 (1999); https://doi.org/10.1063/1.369664

Two dimensional electron gases induced by spontaneous and piezoelectric polarization in undoped and doped AlGaN/GaN heterostructures
Journal of Applied Physics **87**, 334 (2000); https://doi.org/10.1063/1.371866

Control of GaN surface morphologies using plasma-assisted molecular beam epitaxy
Journal of Applied Physics **88**, 1855 (2000); https://doi.org/10.1063/1.1305830

Effect of AlN nucleation layer growth conditions on buffer leakage in AlGaN/GaN high electron mobility transistors grown by molecular beam epitaxy (MBE)

C. Poblenz,[a] P. Waltereit, S. Rajan, U. K. Mishra, and J. S. Speck
Materials Department and Electrical and Computer Engineering Department, University of California, Santa Barbara, California 93106

P. Chin, I. Smorchkova, and B. Heying
Northrop Grumman Space Technology, Redondo Beach, California 90278

(Received 17 February 2005; accepted 2 May 2005; published 21 July 2005)

The effect of the AlN nucleation layer growth conditions on buffer leakage in unintentionally doped AlGaN/GaN high electron mobility transistors was investigated. The samples were grown by rf-plasma assisted molecular beam epitaxy on 4H–SiC (0001). Drain-source leakage currents were found to be markedly different for samples grown with different Al/N flux ratios during the AlN nucleation layer. Growth of N-rich nucleation layers (Al/N <1) resulted in a significant reduction in buffer leakage. Secondary ion mass spectroscopy results showed that Si incorporation into Al-rich AlN layers (Al/N >1) grown on SiC was as high as $\sim 1-2\times 10^{18}$ atoms/cm^3. In contrast, Si incorporation into N-rich AlN layers was two orders of magnitude lower, $\sim 2\times 10^{16}$ atoms/cm^3. Initial devices grown on low-leakage material realized via N-rich nucleation yielded output power densities at 4 GHz of 4.8 W/mm with a power added efficiency (PAE) of 62% at a drain bias of 30 V, and 8.1 W/mm with a PAE of 38% at a drain bias of 50 V. *© 2005 American Vacuum Society.* [DOI: 10.1116/1.1943443]

I. INTRODUCTION

In recent years, AlGaN/GaN high electron mobility transistor structures (HEMTs) have demonstrated very good power performance.[1–5] These devices are promising for microwave power applications due to the high breakdown field and high electron velocity in GaN and because large electron concentrations can be realized in the channel. Growth of a high quality semi-insulating GaN buffer layer is essential for the realization of good device performance and sharp current pinch-off in HEMTs. Unintentionally doped (UID) GaN grown by both metalorganic chemical vapor deposition (MOCVD) and molecular beam epitaxy (MBE) typically exhibits some degree of *n*-type conductivity, presumably due to unintentional oxygen or silicon doping, which can result in buffer leakage in GaN-based electronic devices. In MOCVD GaN growth, iron is used as an intentional deep acceptor to compensate any shallow donors and thus produce highly resistive buffers.[6] Recent approaches by MBE include the introduction of deep acceptors with carbon doping[7–9] or beryllium doping.[10] Our group has recently reported the successful implementation of carbon doping via CBr_4 in GaN to reduce buffer leakage and improve device performance.[11] We also observed, however, that the presence of carbon in the buffer can lead to dispersion effects in HEMTs. Carbon-related trapping effects have also been reported by Klein *et al.*[12] for HEMTs grown by metalorganic vapor-phase epitaxy (MOVPE). Due to the nature of MOVPE growth, some amount of carbon was always present in their films and doping levels were unintentionally varied with growth pressure. This is in contrast to use of CBr_4 for carbon doping during MBE growth, in which case carbon is intentionally incorporated and doping levels are well controlled.[9] In the absence of CBr_4, the carbon levels in our MBE films are negligible. While our previous work established that the free carriers contributing to buffer leakage in AlGaN/GaN/AlN/SiC HEMTs could be successfully compensated with intentional carbon doping in the region near the GaN/AlN interface, the exact origin of the carriers remains unknown.

Recent results from Northrup Grumman Space Technology (NGST)[13] have suggested that variability in buffer leakage currents in AlGaN/GaN/AlN/SiC HEMT structures could be due to the formation of an *n*-type conducting channel in the GaN near the GaN/AlN interface. Silicon incorporation from the SiC substrate was the suggested source of the conducting layer based on secondary ion mass spectroscopy (SIMS) observations. For AlN nucleation layer growth conditions which were nominally stoichiometric (i.e., Al/N $=1$), HEMTs grown with varying AlN nucleation layer thicknesses were investigated. For thin AlN nucleation layers (<50 nm), SIMS showed that Si was present in the AlN and persisted into the subsequent GaN buffer layer. In contrast, for thicker AlN layers (>50 nm), Si incorporation was not found to persist into the GaN buffer. Across a large data set of device measurements, HEMTs with thin AlN nucleation layers resulted in typically high buffer leakage currents, while devices with thick AlN nucleation layers (>50 nm) consistently exhibited lower buffer leakage current. Together with our previous results,[11] this is strong evidence that the

[a]Author to whom correspondence should be addressed; electronic mail: cpoblenz@engineering.ucsb.edu

lower GaN/AlN interface is the region where the buffer leakage is occurring. The NGST results motivated the current work which specifically investigates Si from the SiC substrate as the possible source of conduction in this region. We present here systematic studies of the role of the Al/N flux ratio on impurity incorporation in the AlN nucleation layer and in the GaN near the GaN/AlN interface for UID HEMT structures grown on SiC.

II. EXPERIMENT

The nitride MBE growth reported here was performed in a Varian Gen II MBE system. The active nitrogen was supplied by an AppliedEpi Unibulb rf-plasma source utilizing ultrahigh purity nitrogen (99.9995% purity) which was further purified by an inert gas purifier at the rf-plasma source gas inlet. Conventional effusion cells were used to provide the group III elements. All structures discussed in this article were grown on semi-insulating 4H–SiC substrates commercially available from Cree, Inc. Prior to MBE growth the substrates received a chemical mechanical polish treatment by NovaSiC, Inc. A 0.5 μm titanium film was deposited on the backside of the wafer to provide efficient heat transfer. Quarter-wafer pieces of the substrate were mounted for growth on molybdenum sample holders (nonbonded). The substrate temperature was monitored by an optical pyrometer and the readings were calibrated to the temperature dependence of Ga desorption.[14] Before growth, the substrates were exposed to a "Ga polish" which consisted of three cycles of Ga deposition and desorption to clean the surface from oxides.[15,16] During this process ~21 ML of Ga were deposited at low temperatures (e.g., 670 °C) and subsequently desorbed at high temperatures (e.g., 770 °C). The Ga fluence was well into the regime of Ga droplet formation and ensured that there was complete Ga coverage across the whole wafer regardless of temperature variations. The Ga polish was monitored by reflection high energy electron diffraction (RHEED) and the desorption step was ended when the RHEED pattern was sufficiently bright to indicate desorption of excess Ga and a clear threefold reconstruction from the SiC was observed.

Four HEMT structures were grown to investigate the impact of growth conditions during nucleation on buffer leakage. The nucleation layer consisted of 45 nm AlN grown at 740 °C. Only the Al/N flux ratio during the nucleation layer was varied in the first three structures. The flux ratios utilized were $\mathrm{Al/N}<1$ (sample 1), $\mathrm{Al/N}\approx 1$ (sample 2), and $\mathrm{Al/N}>1$ (sample 3). The fourth sample was also grown with $\mathrm{Al/N}>1$ during nucleation but with the addition of a "drying" step after AlN growth (sample 4). The drying step consisted of closing only the Al shutter, exposing the surface of the AlN to active nitrogen flux and monitoring the surface with reflection high energy electron diffraction (RHEED). The sample was exposed to active nitrogen until the RHEED pattern became significantly bright, indicating consumption of the excess Al through AlN growth.

After AlN growth, the substrate temperature was reduced to ~715 °C for GaN growth. A two-step growth scheme was used to control dislocation density in a similar manner as reported by Manfra *et al.*[17] We have established a buffer growth scheme which allows us to achieve reproducible dislocation densities on the order of $2-3\times 10^{10}$ cm^{-3}, as determined by plan view transmission electron microscopy. Further details on our buffer growth have been published elsewhere.[18] Finally, a 30-nm-thick $\mathrm{Al_{0.30}Ga_{0.70}N}$ cap was deposited. The samples were analyzed using high resolution x-ray diffraction. The cap composition was calculated based on the peak separation between the GaN and AlGaN peaks in 2θ-ω scans assuming coherently strained AlGaN layers.[19] The structural quality of the samples was evaluated utilizing both on-axis x-ray rocking curves, which is an effective means by which to estimate overall dislocation density.[18,20] As the samples were grown near the crossover from the intermediate to Ga-droplet regime,[14] small temperature variations over the sample typically resulted in the formation of Ga droplets in some areas of the sample. After growth, excess Ga and Ga droplets were removed with an HCl etch.

HEMT structures with a drain-source spacing of 3.4 μm, a gate length of 0.7 μm, and gate width of 150 μm were fabricated utilizing standard processing steps. Ohmic contacts consisting of a Ti/Al/Ni/Au metal stack were deposited and alloyed at 870 °C in a nitrogen atmosphere. Mesa isolation was performed using a $\mathrm{BCl_3/Cl_2}$ reactive ion etch, then Ni/Au/Ni gates were deposited. Finally, the samples were passivated using SiN deposited by plasma enhanced CVD and contacts were made to the source, gate, and drain by etching the SiN in a $\mathrm{CF_4}$ plasma. Hall test patterns were not fabricated on the samples presented here, however samples grown under similar conditions exhibited Hall mobilities in excess of 1400 cm^2/V s and sheet carrier concentrations of $\sim 1\times 10^{13}$ cm^{-2}. Buffer leakage was studied by measurement of drain-source *I-V* curves on isolation patterns consisting of HEMT structures with the two-dimensional electron gas etched away at the gate region. To take into account changes in growth conditions across the sample due to variations in substrate temperature, several isolation patterns were measured across each sample and the average result is reported.

Silicon, oxygen, and carbon levels were investigated in three GaN/AlN/SiC structures utilizing SIMS with an 8 keV $\mathrm{Cs^+}$ primary ion beam to etch the samples. The measurements were performed at Charles Evans and Associates, Sunnyvale, CA. The nominal GaN and AlN thicknesses were kept constant at 250 nm. The top GaN layer was grown with $\mathrm{III/V}\geqslant 1$, at or slightly above the crossover to Ga droplet formation in all samples. The Al/N flux ratio during AlN growth was varied from $\mathrm{Al/N}<1$ (sample 1S), $\mathrm{Al/N}\approx 1$ (sample 2S) and $\mathrm{Al/N}>1$ (sample 3S). The AlN growth conditions for SIMS samples 1S, 2S, and 3S correspond directly to the AlN growth conditions used in HEMT samples 1, 2 and 3. Based on RHEED and atomic force microscopy observations of AlN samples grown under the same conditions to the AlN layers in samples 2 and 2S, these layers were grown with an Al wetting layer, and with an Al flux close to the formation of Al droplets.

TABLE I. X-ray diffraction rocking curve FWHMs for HEMT structures with varying Al/N ratios during AlN nucleation layer growth.

SAMPLE	Al/N Ratio	(002) FWHM	(102) FWHM	(201) FWHM
A	Al/N<1	0.052	0.186	0.230
B	Al/N∼1	0.037	0.167	0.203
C	Al/N>1	0.035	0.209	0.282
D	Al/N>1 + N* exposure	0.030	0.188	0.241

III. RESULTS

The full width at half maximums (FWHMs) for both on-axis [(0002)] and off-axis [$(10\bar{1}2)$ and $(20\bar{2}1)$] x-ray rocking curves are shown in Table I for HEMT structures 1–4, grown with varying Al/N ratios during growth of the AlN nucleation layer. Unexpectedly, the overall structural quality was not largely impacted by the changing AlN growth conditions. The average rocking curve FWHMs were 0.039° in (0002), 0.188° in $(10\bar{1}2)$, and 0.239° in $(20\bar{2}1)$. These mosaic values are similar to typical HEMT structures grown with smooth AlN layers (Al/N>1).[18] Figure 1 shows the drain-source *I-V* curves from isolation patterns on each sample in this study. As demonstrated in the figure, samples 2, 3, and 4 (all grown with Al/N⩾1) were extremely leaky. In contrast, sample 1 (grown with Al/N<1) exhibited excellent leakage properties, with buffer leakage as low as samples grown with optimized carbon doping schemes as described in Ref. 11.

To understand the origin of the results shown in Fig. 1, samples 1S, 2S, and 3S (with AlN growth conditions directly corresponding to samples 1, 2 and 3 from Fig. 1) were grown for analysis by SIMS. The Si profiles are shown in Fig. 2 for all three samples. A depth of zero corresponds to the top of the structure. While Al profiles are not shown, they were used to mark the beginning and end of the AlN layers and were abrupt in all samples indicating sharp interfaces. The GaN/AlN interfaces, as determined by the Al SIMS profiles, are indicated in the figure with arrows. As shown in the figure, the AlN layer in sample 1S had a significantly lower Si content than samples 2S or 3S. The Si concentration [Si] in sample 1S was $\sim 2\times10^{16}$ cm^{-3}, whereas for samples 2S and 3S the [Si] was $\sim 1-2\times10^{18}$ cm^{-3} in the AlN. Note that while all three AlN layers were grown for the same amount of time, the AlN in sample 1S was thinner due to the reduced growth rate associated with N-rich growth conditions. A second important feature of the SIMS profiles shown in Fig. 2 is the observation of a spike in Si concentration at the AlN/GaN interface in samples 2S and 3S, and the absence of such a spike in sample 1S.

As buffer leakage is known to degrade transistor performance, devices were fabricated on a low leakage, carbon-free structure (achieved by nucleation layer growth with Al/N<1). Buffer leakage in this structure was on the order of 4 mA/mm drain-source leakage current at 120 V bias. Direct current and small signal measurements were carried out on the device indicating a maximum current of 1 A/mm. The current gain cutoff frequency (f_T) was 21 GHz and the maximum oscillation frequency (f_{MAX}) was 45 GHz. Load-pull measurements at 4 GHz are shown in Fig. 3. An output

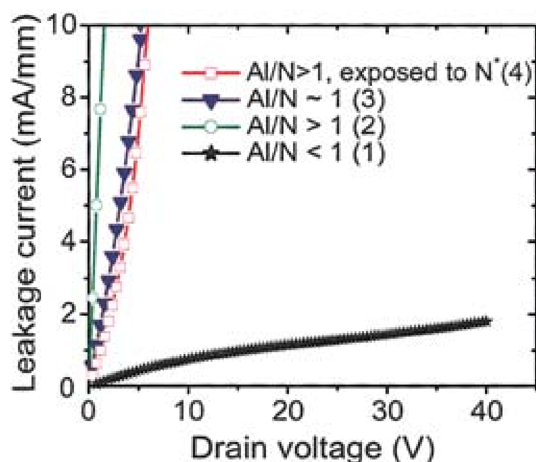

FIG. 1. (Color) Drain-source *I-V* curves for samples 1–4 grown with varying Al/N flux ratios during nucleation as indicated in the figure.

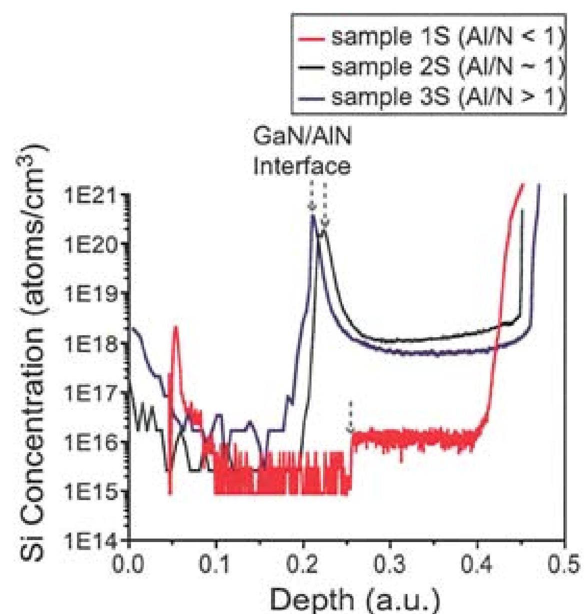

FIG. 2. (Color) Si depth profiles as measured by SIMS for samples 1S, 2S, and 3S.

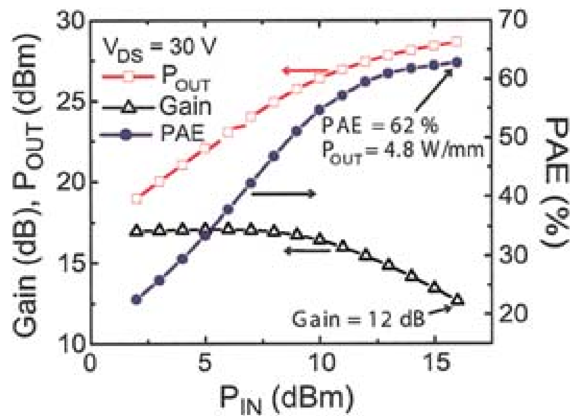

FIG. 3. (Color) Load-pull measurements at 4 GHz for HEMT structures on low-leakage, carbon-free structures.

power density of 4.8 W/mm, power added efficiency (PAE) of 62%, and a gain of 12 dB at a drain bias of 30 V was achieved. An output power density of 8.1 W/mm with 38% PAE was achieved for the same devices at a drain bias of 50 V. These initial device results are promising as the device performance is comparable with low-leakage samples achieved via carbon doping.[21]

IV. DISCUSSION

Recent work on HEMTs with carbon doped buffers[11] has demonstrated that free carriers which contribute to buffer leakage are likely located in the lower part of the HEMT structure. This finding motivated our current work in which the effect of AlN growth conditions on buffer leakage was investigated. Initially, the AlN nucleation layer was investigated due to a suspected region of increased impurity incorporation at the GaN/AlN interface from the presence of excess Al on the surface. Residual Al on the growth surface will be incorporated in preference to Ga in a growing III-nitride layer, thus there may exist a Ga-rich AlGaN layer near the nominal GaN/AlN interface in samples with Al-rich AlN growth. In previous work, we have shown that AlGaN has a markedly higher affinity for oxygen that GaN, even under growth with a complete Ga bilayer.[22] Hence the GaN near the GaN/AlN interface could be unintentionally doped with shallow oxygen donors and thus be conductive. The significant decrease in buffer leakage only for Al-deficient AlN growth demonstrated in Fig. 1 corroborates this idea, although it would be expected that with the addition of a drying step to consume excess Al (sample 4) this could be overcome. However, the GaN buffer for sample 4 also exhibited high leakage. To reconcile this data with the proposed idea of oxygen donors at the GaN/AlN interface, oxygen levels were also examined in the GaN/AlN samples grown for SIMS (samples 1S–3S). Although a specific calibration standard for oxygen was not used, the oxygen levels were estimated to be $\sim 7-10\times 10^{17}$ cm^{-3} in the AlN under all growth conditions. The oxygen profiles were abrupt at the GaN/AlN interface in all samples. In the top GaN layers, the oxygen levels were extremely low ($\sim 4\times 10^{16}$ cm^{-3}), near the background detection limit of the SIMS system ($\sim 2\times 10^{16}$ cm^{-3}). The relatively high level of oxygen in AlN was to be expected based on the aforementioned previous AlGaN results.[22] However, the observation that the oxygen level did not vary with the Al/N flux ratio, or exhibit a spike at the GaN/AlN interface, indicates that oxygen is not the primary source of buffer leakage in subsequent GaN layers and is not associated with the surface coverage of excess Al.

Storm *et al.* have also studied the dependence of buffer leakage on the Al/N flux ratio during growth of underlying AlN nucleation layers. In their work it was also concluded that Al-rich growth of the AlN can result in leaky GaN buffers.[23] While the cause of the increased leakage remains unclear, the trends shown with respect to leakage and Al/N ratio are similar to our results. Recently, Losurdo *et al.* have looked at AlN/SiC interfaces for very thin (10 nm) AlN films using x-ray photoelectron spectroscopy and spectroscopic ellipsometry and note the possible presence of Si–N, Si–O or Si–Si bonds at the interface.[24] In light of previous related work,[13] however, the interaction of metallic Al with the SiC surface was specifically considered here as a potential source of carriers. The Al–Si–C phase diagram shows a range of approximately 6%–24% solubility of Si in liquid Al in equilibrium with SiC at typical MBE growth temperatures (700–750 °C).[25] If the initial AlN growth was performed Al rich, Si could be present and dissolve in the Al wetting layer thus introducing carriers into the AlN or in the GaN near the GaN/AlN interface. This idea was explored in the set of samples measured by SIMS in Fig. 2.

The marked difference in Si incorporation under varying Al/N flux ratios seen in Fig. 2 supports the idea that Si is soluble in the Al wetting layer and will incorporate in AlN during Al-rich AlN growth. The initial stages of Al-rich growth involve a large amount of metallic Al on the surface which can react with the SiC surface. Thus there is potentially a significant amount of Si dissolved in the Al wetting layer which is available to incorporate into the AlN during growth. In the N-rich case, Si from the substrate does not have the opportunity to react with metallic Al, as all Al arriving at the substrate reacts with active N and thus no wetting layer of metallic Al is present on the SiC surface. This is evidenced in Fig. 2 by the two order-of-magnitude difference in Si concentration in the AlN between sample 1S and samples 2S and 3S. Note that the Si profiles for samples 2S and 3S are nearly identical due to the formation of an Al wetting layer during growth of both samples. Therefore the presence of a full Al wetting layer with sparse droplets (sample 2S) and a full wetting layer with dense droplets (sample 3S) had essentially the same effect on Si incorporation, within the experimental error of the SIMS measurements. The reason for the likely formation of a wetting layer even in sample 2S which was grown nominally stoichiometric (Al/N=1) can be understood in light of the AlN growth diagram developed by Koblmüller *et al.*.[26] In their work it was shown that the growth regimes for AlN are essentially equivalent to those observed for GaN growth,[14] with the notable exception that the activation energy for de-

sorption of Al is higher than the activation energy for the desorption of Ga. Thus at typical growth temperatures for GaN (i.e., 700–750 °C) this translates to a greatly reduced intermediate growth regime for AlN growth. Therefore, in practice there is a large probability of forming an Al wetting layer under nominally stoichiometric AlN growth conditions due to temperature or flux distributions across a growing sample.

A second important feature of the SIMS profiles shown in Fig. 2 is the spike in Si concentration at the AlN/GaN interface in samples 2S and 3S, and the absence of this spike in sample 1S. This again supports the idea of a large amount of Si dissolved in the Al wetting layer. For Al-rich growth, the maximum Si concentration in the AlN was $\sim 1-2 \times 10^{18}$ cm^{-3}. The remaining Si was soluble in the Al wetting layer, and likely remained in the Al wetting layer throughout growth and readily incorporated into the initial stages of the subsequent GaN layer. The Si incorporation into GaN is quite high based on the SIMS data (the Si concentration in the spike at the interface exceeds 1×10^{20} cm^{-3}). While the exact order of magnitude of the spike may not be reliable at the interface, a marked increase in Si incorporation here is plausible because it is well known that Si doping levels in excess of 1×10^{19} cm^{-3} can be achieved in GaN. In contrast, for N-rich AlN growth in which there is no Al wetting layer present, little or no amount of Si incorporation in the AlN during growth was observed and no spike in Si concentration was observed at the transition to GaN growth. Thus, Al-rich AlN growth on SiC can enable Si incorporation into AlN and subsequent GaN layers. We do not believe the Al-rich AlN to be conductive, thus GaN buffer leakage in HEMT structures likely results from a thin, highly doped layer of GaN at the GaN/AlN interface. The SIMS mass resolution is sufficiently high such that the Si spikes in the SIMS data are not attributed to mass interference effects.[27]

While the data are not shown here, an additional set of samples was grown to investigate the effect of the pre-growth Ga polish on the Si incorporation in subsequent AlN layers. The sample structures were the same as those which are reported in Fig. 2, however the substrates did not receive a Ga polish prior to growth. These additional experiments were performed because of the apparent reaction of excess Al with the SiC surface at the onset of growth. In the experiments shown in Fig. 2, the surface had already been exposed to several monolayers of Ga prior to AlN growth. With the pre-growth exposure to Ga removed, the SIMS results were identical to those shown in Fig. 2. Thus the Ga reactivity with the SiC surface during the Ga polish was not sufficient to affect the amount of Si incorporation in subsequently grown AlN layers. Oxygen levels in the AlN and GaN layers were also not significantly changed from samples which received the Ga polish.

This work demonstrates that the SiC substrate itself is the likely source of Si in subsequently grown layers, as the initial presence of a liquid Al layer appears to dissolve Si atoms from the SiC surface. Questions therefore remain as to the amount of SiC which is dissolved and where the corresponding C atoms go as a result of this process. Estimation of the number of Si atoms by integration of the SIMS Si profile yields a concentration of Si which is on the order of 1 ML of Si atoms from the SiC substrate. This estimation includes the accumulated Si at the GaN/AlN interface, which contributes a significant amount to the total amount of Si atoms. Thus we recognize that there is error introduced here based on the accuracy of the size and shape of that peak in representing the amount of Si which is dissolved in the Al wetting layer and droplets. Regardless, the presence of the peak in Al-rich samples is compelling evidence that there is some accumulation of Si in the Al wetting layer and droplets, and 1 ML of Si atoms from SiC can introduce a significant Si concentration in the AlN and GaN. The C profiles were also measured by SIMS, revealing similar levels in the AlN in all samples in this study, regardless of Al/N ratio. At present, we do not speculate on the exact level of carbon in these samples due to lack of a proper calibration standard for AlN:C. The carbon levels are low, however, and the data do not indicate that the carbon is dissolved in the wetting layer. Therefore it is likely that only the top layer of Si atoms from the Si-face SiC substrate is affected by the Al at the onset of growth.

The SIMS data presented here correlate well with the leakage data presented in Fig. 1 for varying Al/N flux ratios during AlN nucleation layer growth. All Al-rich samples were leaky (Fig. 1) and corresponding SIMS structures shown in Fig. 2 resulted in high Si incorporation ([Si] $\sim 1-2 \times 10^{18}$ cm^{-3}). Conversely the N-rich sample was the only sample exhibiting low leakage in Fig. 1, and the corresponding SIMS structure in Fig. 2 shows a reduction in Si incorporation by two orders of magnitude. The SIMS data also offer a possible explanation as to why the addition of a drying step to grow out the excess Al did not prevent the subsequent GaN from exhibiting high leakage. If the amount of Si in the Al wetting layer exceeded the Si solubility limit in the growing AlN layer, excess Si would still be present on the surface even if some or all of the Al droplets were consumed with active N exposure. The excess Si would therefore be available to incorporate into the subsequent GaN, and could do so at much higher levels than in the AlN, creating a thin layer of highly doped GaN deep in the buffer. Another possibility is that the AlN layer itself is slightly conducting for Al-rich growth, and this cannot be ruled out based on these experiments. Regardless, compelling evidence for the contribution of Si from the SiC substrate to buffer leakage in MBE-grown HEMTs is provided, as well as a means by which to grow low-leakage GaN buffers without the intentional introduction of compensating centers such as carbon.

V. CONCLUSION

The contribution of varying nucleation conditions to buffer leakage in MBE-grown HEMTs was systematically investigated. It was demonstrated that Al/N flux ratios during growth of AlN nucleation layers on SiC can be tailored to reduce buffer leakage in subsequent GaN layers. Specifically, N-rich growth of AlN nucleation layers was shown to result in subsequent GaN layers with low leakage. Further studies

investigating the source of buffer leakage revealed that there was significant Si incorporation into Al-rich AlN layers grown directly on SiC. Silicon incorporation was shown to be two orders of magnitude lower in AlN nucleation layers grown under N-rich conditions. In addition, accumulated Si at the GaN/AlN interface was shown to result in a thin layer of highly doped GaN at that interface. These results indicate that Si from the SiC substrate is a major contributor to buffer leakage in MBE-grown HEMTs on SiC. Oxygen levels were also measured by SIMS and found to be extremely low in GaN grown on AlN for all AlN growth conditions, indicating that oxygen is not a primary contributor to buffer leakage in the GaN. Device measurements on HEMTs with low drain-source leakage current achieved by Al-deficient nucleation had a power density of 4.8 W/mm with a PAE of 62% at a drain bias of 30 V. These results have significant impact for HEMT growth as understanding and controlling buffer leakage improves device performance. In addition, initial results were presented which indicate leakage can be controlled in UID material, potentially eliminating the need for introducing intentional compensating centers such as carbon which can have other effects on device performance such as dispersion.

ACKNOWLEDGMENTS

The authors acknowledge financial support from DARPA (Edgar Martinez and Mark Rosker, Program Managers) managed by ONR (Harry Dietrich, Contract Monitor). This work made use of the MRL Central Facilities supported by the MRSEC Program of the National Science Foundation under Award No. DMR00-80034.

[1] H. Xing, S. Keller, Y. F. Wu, L. McCarthy, I. P. Smorchkova, D. Buttari, R. Coffie, D. S. Green, G. Parish, S. Heikman, L. Shen, N. Zhang, J. J. Xu, B. P. Keller, S. P. DenBaars, and U. K. Mishra, J. Phys.: Condens. Matter **13**, 7139 (2001).
[2] R. Behtash, H. Tobler, M. Neuburger, A. Schurr, H. Leier, Y. Cordier, F. Semond, F. Natali, and J. Massies, Electron. Lett. **39**, 626 (2003).
[3] J. S. Moon, M. Micovic, P. Janke, P. Hashimoto, W.-S. Wong, R. D. Widman, L. McCray, A. Kurdoghlian, and C. Nguyen, Electron. Lett. **37**, 528 (2001).
[4] D. S. Katzer, S. C. Binari, D. F. Storm, J. A. Roussos, B. V. Shanabrook, and E. R. Glaser, Electron. Lett. **38**, 1740 (2002).
[5] N. Weimann, M. J. Manfra, and R. Wachtler, IEEE Electron Device Lett. **24**, 57 (2003).
[6] S. Heikman, S. Keller, S. P. DenBaars, and U. K. Mishra, Appl. Phys. Lett. **81**, 439 (2002).
[7] H. Tang, J. B. Webb, J. A. Bardwell, S. Raymond, J. Salzman, and C. Uzan-Saguy, Appl. Phys. Lett. **78**, 757 (2001).
[8] J. B. Webb, H. Tang, S. Rolfe, and J. A. Bardwell, Appl. Phys. Lett. **75**, 953 (1999).
[9] D. S. Green, U. K. Mishra, and J. S. Speck, J. Appl. Phys. **95**, 8456 (2004).
[10] D. S. Katzer, D. F. Storm, S. C. Binari, J. A. Roussos, B. V. Shanabrook, and E. R. Glaser, J. Cryst. Growth **251**, 481 (2003).
[11] C. Poblenz, P. Waltereit, S. Rajan, S. Heikman, U. K. Mishra, and J. S. Speck, J. Vac. Sci. Technol. B **22**, 1145 (2004).
[12] P. B. Klein, S. C. Binari, K. Ikossi, A. E. Wickenden, D. D. Koleske, and R. L. Henry, Appl. Phys. Lett. **79**, 3527 (2001).
[13] P. Chin, I. Smorchkova, and B. Heying, Northrup Grumman Space Technology, Redondo Beach, CA (unpublished).
[14] B. Heying, R. Averbeck, L. F. Chen, E. Haus, H. Riechert, and J. S. Speck, J. Appl. Phys. **88**, 1855 (2000).
[15] O. Brandt, R. Muralidharan, P. Waltereit, A. Thamm, A. Trampert, H. von Kiedrowski, and K. H. Ploog, Appl. Phys. Lett. **75**, 4019 (1999).
[16] S. Wright and H. Kroemer, Appl. Phys. Lett. **36**, 210 (1980).
[17] M. J. Manfra, N. G. Weimann, J. W. P. Hsu, L. N. Pfeiffer, K. W. West, and S. N. G. Chu, Appl. Phys. Lett. **81**, 1456 (2002).
[18] P. Waltereit, C. Poblenz, S. Rajan, F. Wu, J. S. Speck, and U. K. Mishra, Jpn. J. Appl. Phys., Part 2 **43**, L1520 (2004).
[19] A. Saxler, P. Debray, R. Perrin, S. Elhamri, W. C. Mitchel, C. R. Elsass, I. P. Smorchkova, B. Heying, E. Haus, P. Fini, J. P. Ibbetson, S. Keller, P. M. Petroff, S. P. DenBaars, U. K. Mishra, and J. S. Speck, J. Appl. Phys. **87**, 369 (2000).
[20] B. Heying, X. H. Wu, S. Keller, Y. Li, D. Kapolnek, B. P. Keller, S. P. DenBaars, and J. S. Speck, Appl. Phys. Lett. **68**, 643 (1996).
[21] S. Rajan, P. Waltereit, C. Poblenz, S. Heikman, D. S. Green, J. S. Speck, and U. K. Mishra, IEEE Electron Device Lett. **25**, 247 (2004).
[22] C. R. Elsass, T. Mates, B. Heying, C. Poblenz, P. Fini, P. M. Petroff, S. P. DenBaars, and J. S. Speck, Appl. Phys. Lett. **77**, 3167 (2000).
[23] D. F. Storm, D. S. Katzer, S. C. Binari, B. V. Shanabrook, L. Zhou, and D. J. Smith, Appl. Phys. Lett. **85**, 3786 (2004).
[24] M. Losurdo, P. Capezzuto, G. Bruno, A. Brown, T. H. Kim, C. Yi, D. N. Zakharov, and Z. Liliental-Weber, Appl. Phys. Lett. **86**, 021920 (2005).
[25] V. Laurent, D. Chatain, and N. Eustathopoulos, J. Mater. Sci. **22**, 244 (1987).
[26] G. Koblmüller, R. Averbeck, L. Geelhaar, H. Riechert, W. Hösler, and P. Pongratz, J. Appl. Phys. **93**, 9591 (2003).
[27] Charles Evans and Associates, Sunnyvale, CA (private communication).